



Published in final edited form as:

Int J Radiat Oncol Biol Phys. 2018 November 15; 102(4): 1357–1365. doi:10.1016/j.ijrobp.2018.07.186.

Interim Analysis of a Two-Institution, Prospective Clinical Trial of 4DCT-Ventilation-based Functional Avoidance Radiation Therapy

Yevgeniy Vinogradskiy, PhD^{*}, Chad G. Rusthoven, MD^{*}, Leah Schubert, PhD^{*}, Bernard Jones, PhD^{*}, Austin Faught, PhD[†], Richard Castillo, PhD[‡], Edward Castillo, PhD[§], Laurie E. Gaspar, MD, MBA^{*}, Jennifer Kwak, MD^{||}, Timothy Waxweiler, MD^{*}, Michele Dougherty, PhD[¶], Dexiang Gao, PhD[#], Craig Stevens, MD, PhD[§], Moyed Miften, PhD^{*}, Brian Kavanagh, MD, MPH^{*}, Thomas Guerrero, MD, PhD[§], Inga Grills, MD[§]

^{*}Department of Radiation Oncology, University of Colorado School of Medicine, Aurora, Colorado;

[†]Department of Radiation Oncology, St Jude Children's Research Hospital, Memphis, Tennessee;

[‡]Department of Radiation Oncology, Emory University, Atlanta, Georgia;

[§]Department of Radiation Oncology, Beaumont Health System, Royal Oak, Michigan;

^{||}Department of Radiology, University of Colorado School of Medicine, Aurora, Colorado;

[¶]Department of Radiation Oncology, Mayo Clinic, Rochester, Minnesota;

[#]Department of Pediatrics and Department of Biostatistics and Informatics, University of Colorado School of Medicine, Aurora, Colorado

Abstract

Purpose: Functional imaging has been proposed that uses 4DCT images to calculate 4DCT-based lung ventilation (4DCT-ventilation). We have started a 2-institution, phase 2 prospective trial evaluating the feasibility, safety, and preliminary efficacy of 4DCT-ventilation functional avoidance. The trial hypothesis is that the rate of grade 2 radiation pneumonitis could be reduced to 12% with functional avoidance, compared with a 25% rate of pneumonitis with a historical control. The trial employed a Simon 2-stage design with a planned futility analysis after 17 evaluable patients. The purpose of this work is to present the trial design and implementation, dosimetric data, and clinical results for the planned futility analysis.

Methods and Materials: Eligible patients were patients with lung cancer who were prescribed doses of 45 to 75 Gy. For each patient, the 4DCT data were used to generate a 4DCT-ventilation image using the Hounsfield unit technique along with a compressible flow-based image registration algorithm. Two intensity modulated radiation therapy treatment plans were generated: (1) a standard lung plan and (2) a functional avoidance treatment plan that aimed to reduce dose to functional lung while meeting target and normal tissue constraints. Patients were treated with the functional avoidance plan and evaluated for thoracic toxicity (presented as rate and 95% confidence intervals [CI]) with a 1-year follow-up.

Reprint requests to: Yevgeniy Vinogradskiy, PhD, Department of Radiation Oncology, University of Colorado School of Medicine, Aurora, Colorado 80045. Tel: (720) 848-0157; yevgeniy.vinogradskiy@ucdenver.edu.

Supplementary material for this article can be found at <https://doi.org/10.1016/j.ijrobp.2018.07.186>.

Results: The V20 to functional lung was $21.6\% \pm 9.5\%$ (mean \pm standard deviation) with functional avoidance, representing a decrease of 3.2% ($P < .01$) relative to standard, nonfunctional treatment plans. The rates of grade 2 and grade 3 radiation pneumonitis were 17.6% (95% CI, 3.8%–43.4%) and 5.9% (95% CI, 0.1%–28.7%), respectively.

Conclusions: Dosimetrically, functional avoidance achieved reduction in doses to functional lung while meeting target and organ at risk constraints. On the basis of Simon's 2-stage design and the 17.6% grade 2 pneumonitis rate, the trial met its futility criteria and has continued accrual.

Summary

Functional avoidance has been proposed as a means of using functional imaging to reduce the dose to functional regions of the lung in order to reduce thoracic toxicity. We have started a 2-institution, early-phase clinical trial to use a novel lung functional imaging modality (termed 4-dimensional computed tomography—ventilation) for functional avoidance radiation therapy. The purpose of this work is to present the trial design and implementation, dosimetric results, and an interim clinical toxicity analysis.

Introduction

A form of functional imaging has been developed that uses 4-dimensional computed tomography (4DCT) or breath-hold computed tomography (CT) images to calculate regional change in air content, which can be considered a surrogate for ventilation (referred to as 4DCT-ventilation). For patients who undergo 4DCT imaging during the planning process to aid with breathing motion management during radiation therapy (1), calculating functional imaging with 4DCT-ventilation does not burden the patient with an extra imaging procedure. 4DCT-ventilation has several potential advantages over nuclear medicine ventilation-perfusion (VQ) imaging, which is currently the clinical standard for ventilation imaging. Compared with nuclear medicine VQ scans, 4DCT-ventilation is a faster imaging procedure, does not require an inhaled radioactive aerosol, does not have an artifact where the aerosol gets stuck in the airway (2), has improved spatial resolution, and is by definition an imaging modality that provides both anatomic (4DCT) and functional (4DCT-ventilation) information. The concept of 4DCT-ventilation has progressed from a research idea to an imaging modality being investigated in the prospective setting. Early 4DCT-ventilation work focused on developing the methodology for generating 4DCT-ventilation images (3–7) and validating the generated images against other forms of lung function imaging (2, 8–11) and pulmonary function test (PFT) data (9, 12).

The main clinical application of 4DCT-ventilation is for functional avoidance radiation therapy, which implies generating radiation treatment plans that aim to avoid functional portions of the lung (as measured by 4DCT-ventilation) (13–15). The idea is that reducing dose to functional regions of lung can reduce the rate of thoracic side effects from radiation treatment (13, 16). Functional avoidance has been proposed using 4DCT-ventilation (14, 17) and other imaging modalities (18), including single-photon emission computed tomography (19, 20), positron emission tomography, (21) and ^3He -magnetic resonance imaging (22). The hypothesis that reducing the dose to the functional lung can reduce the probability that patients will develop radiation pneumonitis or fibrosis has been supported in retrospective

modeling studies (13, 23–25). By using a retrospective study of 70 patients, recent work has shown that including 4DCT-ventilation functional information in the planning process can reduce the probability of grade 2 pneumonitis by 5% on average and by as much as 20% for individual patients (23).

Several institutions (,) are beginning to evaluate 4DCT-ventilation functional avoidance in the prospective setting (26). We have started a 2-institution, phase 2 prospective clinical trial evaluating the feasibility, safety, and preliminary efficacy of 4DCT-ventilation functional avoidance (). The rationale for electing a phase 2 study design was to evaluate the feasibility of incorporating 4DCT-ventilation-based functional avoidance in a clinical environment and to determine whether 4DCT-ventilation should be considered for a larger-scale, randomized study. The primary endpoint of the study is to compare symptomatic, grade 2 radiation pneumonitis rates against a historical control by using pneumonitis rates estimated from the Quantitative Analyses of Normal Tissue Effects in the Clinic (QUANTEC) lung report (27). The purpose of this work is to present an interim analysis of the 2-institution, 4DCT-ventilation functional avoidance clinical trial. Specifically, we report on trial design and implementation, dosimetric results, and a planned futility analysis of clinical toxicity.

Methods and Materials

Inclusion and exclusion criteria

The study was approved to enroll patients by the institutional review boards at the University of Colorado (Aurora, CO) and Beaumont Health System (Royal Oak, MI) (). Written informed consent was obtained from each patient before study enrollment. All data were anonymized and maintained in a password-protected REDCap secure web application. Inclusion criteria included diagnosis of pathologically confirmed lung cancer, age ≥ 18 years, and a planned concurrent chemotherapy regimen. The criteria for needing to have a planned concurrent chemotherapy regimen was included to help homogenize the study population. Patients must have received a definitive course of radiation therapy, which was defined as prescription dose of 45 to 75 Gy. Patients were excluded if they were being treated with stereotactic body radiation therapy (SBRT) (defined as <5 fractions) or if they were receiving palliative treatment (defined as <45 Gy). Although 4DCT-ventilation may have a potential benefit for patients treated with SBRT (28), SBRT was excluded from the study because of the differing toxicity profiles of patients receiving SBRT treatment (compared with patients receiving treatment with standard fractionation) and because of the unique treatment planning demands of SBRT. The overall rationale for the early-phase trial inclusion and exclusion criteria was to enable evaluation of a wide set of clinical scenarios, including patients with both small cell lung cancer (SCLC) and non-small cell lung cancer (NSCLC) as well as patients with a wide variety of disease staging.

4DCT imaging, 4DCT-ventilation generation, and 4DCT-ventilation image assessment

Each patient enrolled on the study underwent a 4DCT simulation as part of the treatment planning process. The 4DCT was performed on either a Siemens Somatom (Siemens Healthcare, Tarrytown, NY) or a Philips Brilliance Big Bore CT. A gated lung protocol was used on both scanners with 120 kVp, 3-mm slices, and variable mAs. Image reconstruction

was done using standard filtered back projection algorithms commercially available on both scanners. CT images were binned to create a 4DCT image using phase-based sorting methods and the commercially available sorting algorithms on both scanners. A physicist reviewed each 4DCT to ensure consistent patient breathing and minimal motion artifact on the 4DCT images.

The Hounsfield unit calculation technique (3, 4, 29) was used to calculate a ventilation image for each patient from the 4DCT data. The first step of the calculation is to use a deformable image registration algorithm to map lung voxel elements between the inhale and exhale phases (30). The spatial accuracy of the deformable image registration algorithm used for the study was found to be 1.25 mm for thoracic registrations (30). The lungs are segmented in a semiautomated algorithm to delineate the trachea, bronchi, and pulmonary vasculature (3). Once the inhale and exhale voxels are linked and the lungs are delineated, a density-change—based equation is applied to calculate ventilation (4, 31):

$$\frac{V_{in} - V_{ex}}{V_{ex}} = 1000 \frac{HU_{in} - HU_{ex}}{HU_{ex}(1000 + HU_{in})} \quad (1)$$

where V_{in} and V_{ex} are the inhale and exhale volumes and HU_{in} and HU_{ex} are the inhale and exhale Hounsfield units of the individual lung voxels. Equation 1 calculates the local change in air content for each voxel and produces a 3-dimensional map of a surrogate of ventilation (Fig. 1).

The trial employed 4DCT-ventilation image heterogeneity inclusion criteria. The rationale for the imaging-based inclusion criteria is that if a patient has homogenous lung function, there are no regions to preferentially spare. Conversely, if a patient's ventilation image is heterogeneous and displays a major ventilation defect, functional avoidance can be used to spare functional portions of the lung by preferentially depositing dose in the defect area. Because of a lack of data for determining 4DCT-ventilation image heterogeneity criteria, we instituted both quantitative and qualitative imaging criteria. To be eligible for the study, the patient's 4DCT-ventilation image had to have (1) a ventilation defect noted (scored as a binary yes or no) by the radiation oncologist and (2) a 15% reduction in regional lung function. The algorithm for evaluating the 4DCT-ventilation image for a 15% reduction in regional lung function has been previously described (32, 33). The algorithm employs a technique adapted from VQ scans in which the lungs are divided into geometric-thirds (34) and evaluates whether the ventilation defect occurs in a geometric-third around the tumor. The radiation oncologist's interpretation of the 4DCT-ventilation image for a ventilation defect was meant to provide clinically pertinent additional inclusion criteria.

4DCT-ventilation functional avoidance treatment planning and radiation treatment

The functional treatment planning process employed a structure-based treatment planning approach. The structure-based approach uses the 4DCT-ventilation image to create a functional avoid contour and has been demonstrated with 4DCT-ventilation along with other lung function imaging modalities (14, 15, 22, 35–38). The functional avoid contour represents the functional regions of the lung and is used for preferential avoidance. The functional avoid contour was created by autosegmenting regions of the 4DCT-ventilation

image using a lower threshold of 15%, which was determined from previous retrospective studies (32, 33).

For each patient, 2 treatment plans were generated: (1) a standard lung plan with no functional information incorporated (referred to as the nonfunctional plan) and (2) a functional avoidance treatment plan. The treatment planner first generated the nonfunctional plan and subsequently used the nonfunctional plan as a baseline to generate the functional avoidance plan. The planners were instructed to prioritize (1) delivering the prescribed dose to the planning target volume (PTV), (2) meeting standard thoracic organ at risk (OAR) constraints, and (3) reducing dose to the functional avoid contour. Prioritizing PTV coverage and standard OAR constraints before reducing dose to functional lung ensured that all the functional avoidance plans met standard thoracic planning criteria.

Planning criteria for the PTV coverage and OAR constraints were at the discretion of the treating physician and generally followed Radiation Therapy Oncology Group (RTOG) 0617 for NSCLC and RTOG 0538 for SCLC. OARs were contoured for the lungs (excluding gross tumor volume), heart, esophagus, and spinal cord, as well as the liver, brachial plexus, and great vessels when pertinent to the treatment plan. Both the nonfunctional and functional plans used rotational intensity modulated radiation therapy (IMRT) techniques and had to meet the prescribed PTV coverage and OAR constraints. Functional avoidance dosimetric results are presented (result shown as mean \pm standard deviation) for the PTV coverage, PTV hotspot, standard OAR metrics, and achieved metrics for the functional avoid structure. The dosimetric results for the nonfunctional plans are reported to quantify the reduction in dose to functional lung with functional avoidance planning. The dosimetric results are compared for the functional and nonfunctional plans using *t* tests. Further treatment planning details (including treatment planning systems, dose calculation algorithms, rationale for creating nonfunctional plans, and further dosimetric details) are provided in Appendix E1 (available online at <https://doi.org/10.1016/j.ijrobp.2018.07.186>).

Image guidance required a daily cone beam image to align the patient. Adaptive replanning criteria were left up to the treating physician. Because studies have noted that lung reventilation and reperfusion is possible as the tumor shrinks (29) if the patient required resimulation and replanning, another 4DCT image was acquired, and the adaptive replan incorporated the 4DCT-ventilation image generated from the resimulation 4DCT.

Trial quality assurance procedures

Several quality assurance (QA) procedures were put in place specific to 4DCT-ventilation functional avoidance. Measures were taken to ensure consistent 4DCT-ventilation calculations between the 2 centers. Exact versions of the 4DCT-ventilation software were installed at both centers. A site initiation visit (SIV) was performed in which physicists from the coordinating center performed official training of the 4DCT-ventilation calculation techniques and provided examples of functional avoidance treatment plans. Three 4DCT-ventilation sample calculations cases were performed and compared between the 2 centers to ensure consistent 4DCT-ventilation calculations. Only physicists who were training during the SIV were allowed to perform the trial 4DCT-ventilation calculations. For each enrolled patient, regardless of the enrolling institution, the same physicist would double-check all of

the 4DCT-ventilation calculations. As part of the SIV, 3 sample functional avoidance cases were planned at both centers and qualitatively compared to ensure consistent functional avoidance planning techniques.

Sample size calculations and trial outcome assessments

The primary trial outcome measure was clinical toxicity using the National Cancer Institute Common Terminology Criteria for Adverse Events (version 4). Clinical toxicity was assessed before treatment; weekly during treatment; at the end of treatment; and 3, 6, and 12 months after treatment. The primary endpoint of the trial was the rate of grade 2 (symptomatic) radiation pneumonitis, to be compared against a historical control of a 25% rate of symptomatic pneumonitis.

The 25% rate of grade 2 pneumonitis to be used as a historical control was estimated from the QUANTEC lung report (27), which was considered the most pertinent estimate of toxicity at the time of trial design. The trial hypothesis was that the crude rate of grade 2 radiation pneumonitis could be reduced to 12% with functional avoidance, compared with the 25% rate of pneumonitis with a historical control. The trial's planned enrollment was a total of 67 evaluable patients. Patients were considered evaluable if they had at least a 3-month follow-up. Using a Simon's 2-stage optimum design (39) with an undesirable grade 2 radiation pneumonitis-free rate of 75% (25% rate of grade 2 pneumonitis rate to be used as a historical control) and a desirable grade 2 pneumonitis-free rate of 88% (12% rate of grade 2 pneumonitis with functional avoidance), 67 patients would provide a study power of 80% with a type I error rate of 0.05. Seventeen evaluable patients would be recruited during the first stage. The study would be stopped for futility if 4 of 17 patients had grade 2 pneumonitis; otherwise, the trial would proceed to recruit an additional 50 evaluable patients during the second stage.

In addition to pneumonitis, other thoracic toxicities were recorded, including esophagitis, cough, dyspnea, and fatigue. Although not assessed in this interim analysis, the trial includes secondary outcome measures using thoracic quality-of-life questionnaires, PFTs, and imaging-based endpoints. We present crude toxicity results for the 17-patient interim analysis cohort along with accompanying exact 95% confidence intervals (CIs).

Results

To get 17 evaluable patients, 24 patients were enrolled. One patient (6%) was considered a screen fail as a result of not meeting 4DCT-ventilation image heterogeneity criteria, 2 patients were considered screen fails because of not receiving concurrent chemotherapy, and 1 patient withdrew from the study. Of the remaining 20 patients, 17 were evaluable. The clinical parameters for the evaluable 17-patient cohort are shown in Table 1. The study population was 76% female and 24% male. Thirty-five percent of patients had chronic obstructive pulmonary disease, 29% had prior lung surgery (4 lobectomies and 1 wedge resection), 94% were current or former smokers, and the median Karnofsky Performance Status score was 90 (range, 80–100). The split between NSCLC and SCLC was 71% and 29%, respectively, and 82% of patients on the study had stage IIIA or IIIB disease.

The prescription doses for the study cohort were 45 Gy in 30 fractions twice daily (23%), 50 Gy in 25 fractions (12%), 50.4 Gy in 28 fractions (12%), and 60 Gy in 30 fractions (53%). The dosimetric parameters for the functional avoidance clinical plans are shown in Table 2. The mean lung dose and lung V20 (volume of lung receiving 20 Gy) were 14.4 ± 3.4 Gy and $24.5\% \pm 7.2\%$, respectively. The mean dose to the functional avoidance structure was 13.4 ± 3.8 Gy with functional planning and 14.8 ± 3.3 Gy with nonfunctional planning for a significant ($P < .01$) difference of 1.4 Gy (range, 0.3–3.6 Gy). Similarly, the V20 to the functional avoidance structure was $21.6\% \pm 9.5\%$ with functional planning and $24.8\% \pm 9.4\%$ with nonfunctional planning for a significant ($P < .01$) reduction of 3.2% (range, 0.1%–7.9%). A representative case of a patient with larger reductions in dose to the functional avoidance (compared with nonfunctional planning) is shown in Figure 2. The PTV coverage was $95.0\% \pm 4.5\%$ with functional planning, which was significantly ($P = .04$) lower than the $96.0\% \pm 5.7\%$ PTV coverage with nonfunctional planning. The maximum spinal cord dose was significantly ($P = .05$) higher with functional planning (34.9 ± 7.9 Gy) than with nonfunctional planning (33.6 ± 33.6 Gy).

The thoracic toxicity data are summarized for any grade 1, 2, or 3 toxicity (no grade 4 or higher thoracic toxicities were observed) in Table 3. The median follow-up time for the presented toxicity results was 10 months (range, 4–12 months). At the first stage, 3 of the 17 patients experienced grade 2 radiation pneumonitis, thus meeting the criteria for proceeding to the second stage. The rates of grade 2 and grade 3 radiation pneumonitis were 17.6% (95% CI, 3.8%–43.4%) and 5.9% (95% CI, 0.1%–28.7%), respectively. In terms of timing, the 3 grade 2 pneumonitis events occurred at 3 months, 4 months, and 5 months after the completion of radiation treatment. The rate of grade 2 and grade 3 esophagitis was 47.1% (95% CI, 23.0%–72.2%) and 11.8% (95% CI, 1.5%–36.4%), respectively. Eighteen percent of patients (95% CI, 3.8%–43.4%) experienced a grade 3 thoracic toxicity of any kind.

Discussion

On the basis of Simon's 2-stage design and the 17.6% grade 2 pneumonitis rate, the trial met its futility criteria and has continued accrual. The trial was designed to be compared against a historical control, and at the time of study design, the QUANTEC lung report provided the most pertinent historical comparison. It is likely that toxicity rates have improved since the QUANTEC report was published, and it is instructive to review pneumonitis rates with more recent work, in which modern treatment planning and delivery advances (most importantly IMRT) are incorporated.

Single-institution reports for patients treated with IMRT cite grade 2 pneumonitis rates of 18% (40) and grade 3 rates of 8 to 12.5% (40–43). RTOG 0617 evaluated NSCLC patients (44, 45) treated with 60 Gy versus 74 Gy and reported rates of grade 3 radiation pneumonitis, pulmonary events, and esophagitis of 7%, 20%, and 7%, respectively, in the 60-Gy arm (44). When the RTOG 0617 analysis was restricted to patients treated with IMRT, the rate of grade 3 radiation pneumonitis was 3.5%, and the rate of grade 3 esophagitis was 13.2% (45).

It should be emphasized that the interim toxicity results from our single-arm study should be interpreted with caution relative to RTOG 0617 because there are several notable population differences between the studies. Because we were performing an early-phase trial, our inclusion and exclusion criteria were by design not restrictive and created a heterogeneous study population. Our study included patients with SCLC in addition to patients with NSCLC, whereas RTOG 0617 included only patients with NSCLC. Pneumonitis rates for SCLC have been reported to be 2% to 6.2% (46, 47). Our study did not include any restrictions on performance status or pretreatment pulmonary function, while RTOG 0617 incorporated performance status and PFT-based inclusion criteria. Our study allowed enrollment of patients who had undergone previous re-sections to treat their lung cancer, while RTOG 0617 enrolled patients whose disease was unresectable. Although treatment planning objectives generally followed RTOG 0617 and RTOG 0538 planning guidelines, the final objectives were at the discretion of the treating physician. The variability in the planning guidelines has the potential to affect the toxicity rates with functional avoidance.

One of the goals of the early-phase trial was to evaluate the feasibility and practical implementation of functional avoidance. Both the image heterogeneity and the dosimetry results are presented as means to evaluate feasibility by identifying the patients for whom functional avoidance can potentially make the largest dosimetric impact and quantifying the magnitude of the dosimetric improvement to functional lung for the identified cohort. Our study determined that 94% of patients met the image heterogeneity criteria, which is higher than the previously reported rate of 70%. (33) The presented 3.2% reduction in V20 to the functional avoidance structure with functional planning is in the range reported by a review article, which cited reductions between “no significant difference” and 5% for CT-based methods, 3% to 7% using single-photon emission computed tomography, and 2% to 3% reductions with magnetic resonance imaging (18). Despite the image heterogeneity criteria, which was intended to exclude patients who do not have conducive functional profiles, there was still a wide range in how much dosimetric benefit was achieved from functional avoidance. For example, the reductions in V20 to functional lung ranged from 0.1% to 7.9% (Table 2). The largest improvement in functional V20 occurred in patients for whom the 4DCT-ventilation image provided information that altered the gantry start-and-stop angles for the rotational IMRT plan. Evaluation of the ongoing clinical trials will need to be done to identify parameters that can better predict for patients who will receive a dosimetric (and clinical) benefit with functional avoidance.

Retrospective studies have shown that as the treatment planning system is pushed to reduce dose to functional lung, other plan quality metrics can suffer (15, 35, 48). Our study noted a statistically significant decrease of 1.0% in PTV coverage and a 1.3-Gy increase in maximum spinal cord dose with functional avoidance planning compared with nonfunctional planning (Table 2). Both the PTV coverage decrease to 95.0% and the spinal cord maximum dose increase to 34.9 Gy with functional planning resulted in plans that were considered within acceptable clinical limits at both institutions. As with other technologically intensive clinical treatments, functional avoidance demands greater resources, oversight, and QA measures. A greater emphasis was applied to evaluating the patient’s 4DCT because the quality of the 4DCT can have an impact on the quality of the generated 4DCT-ventilation image (49). Overall, we estimate that the extra oversight, QA, and dosimetric complexity

with functional avoidance in our study requires an extra 1.5 hours per patient for both the physicist and the dosimetrist. We believe 4DCT-ventilation functional avoidance will be assessed in a fashion similar to adaptive radiation therapy as the dosimetric (and clinical) gains for each patient will be evaluated against dosimetric and resource limitations.

Several uncertainties and limitations are important to note regarding 4DCT-ventilation in the context of functional avoidance. Our study reports crude pneumonitis rates, with patients being considered evaluable if they have completed the 3-month follow-up visit with the radiation oncologist. Three months was chosen as the time point to consider patients evaluable because of practical considerations in limiting the number of patients who are lost because of follow-up. The crude grade 2 radiation pneumonitis rate was chosen as the binary endpoint to facilitate comparison with historical controls because crude rates are more frequently reported in the literature than actuarial rates. However, crude rates of pneumonitis underestimate the true toxicity rates because patients who are lost to follow-up may develop toxicity. For the final trial analysis, in addition to reporting crude toxicity rates, actuarial rates will be presented using the Kaplan-Meier method (50). The calculation techniques for 4DCT-ventilation are still being optimized (11), which includes methods to deal with 4DCT imaging artifacts, deformable image registration uncertainties (51), and variation in patient breathing effort (52). Studies comparing 4DCT-ventilation to other forms of lung function imaging have demonstrated mixed correlation coefficients because of artifacts in both 4DCT-ventilation and other lung function imaging modalities (18, 53). Studies have noted that ventilation can potentially improve throughout treatment if the tumor shrinks and the airways open up (29), making an adaptive approach important for functional avoidance. Our adaptive approach employs functional replanning in situations in which an adaptive plan was required. Other studies have incorporated a scheduled midtreatment 4DCT-ventilation scan to verify the spatial ventilation distribution. A shortcoming of 4DCT-ventilation compared with VQ scans is that no perfusion data are provided. A recent review article on functional avoidance (18) noted that perfusion data may be more pertinent than ventilation when performing functional avoidance because perfusion has been shown to be a more sensitive metric for assessing lung function. The results of the ongoing functional avoidance clinical trials assessing both ventilation and perfusion will help determine whether ventilation or perfusion is more critical in reducing toxicity.

Conclusions

The current work presents the trial design and implementation, dosimetric data, and an interim futility analysis for 17 patients enrolled on a 4DCT-ventilation functional avoidance clinical trial. Functional avoidance reduced the mean dose to functional lung by 1.4 Gy and V20 by 3.2% (compared with nonfunctional plans) while meeting PTV coverage and OAR constraints. The rate of grade 2 and 3 radiation pneumonitis for the interim analysis for functional avoidance was 17.6% and 5.9%, respectively, which met the trial interim futility analysis criteria.

Supplementary Material

Refer to Web version on PubMed Central for supplementary material.

Acknowledgments

This work was funded by grant R01CA200817 (Y.V., L.S., J.K., M.M., B.K., E.C., R.C., T.G.).

References

1. National Comprehensive Cancer Network. Non-small cell lung cancer. NCCN Guidelines, version 3.2012; 2012 Available at: https://www.nccn.org/professionals/physician_gls/recently_updated.aspx. Accessed April 21, 2016.
2. Castillo R, Castillo E, McCurdy M, et al. Spatial correspondence of 4D CT ventilation and SPECT pulmonary perfusion defects in patients with malignant airway stenosis. *Phys Med Biol* 2012;57:1855–1871. [PubMed: 22411124]
3. Castillo R, Castillo E, Martinez J, et al. Ventilation from four-dimensional computed tomography: Density versus jacobian methods. *Phys Med Biol* 2010;55:4661–4685. [PubMed: 20671351]
4. Guerrero T, Sanders K, Castillo E, et al. Dynamic ventilation imaging from four-dimensional computed tomography. *Phys Med Biol* 2006;51:777–791. [PubMed: 16467578]
5. Reinhardt JM, Ding K, Cao K, et al. Registration-based estimates of local lung tissue expansion compared to xenon CT measures of specific ventilation. *Med Image Anal* 2008;12:752–763. [PubMed: 18501665]
6. Yamamoto T, Kabus S, von Berg J, et al. Four-dimensional computed tomography-based pulmonary ventilation imaging for adaptive functional guidance in radiotherapy. *J Thorac Oncol* 2009;4:S959–S960.
7. Kipritidis J, Siva S, Callahan J, et al. Strong evidence for physiologic correlation of 4D-CT ventilation imaging with respiratory-correlated gallium 68 PET/CT in humans. *Med Phys* 2013;40:424.
8. Vinogradskiy Y, Koo PJ, Castillo R, et al. Comparison of 4-dimensional computed tomography ventilation with nuclear medicine ventilation-perfusion imaging: A clinical validation study. *Int J Radiat Oncol Biol Phys* 2014;89:199–205. [PubMed: 24725702]
9. Yamamoto T, Kabus S, Lorenz C, et al. Pulmonary ventilation imaging based on 4-dimensional computed tomography: Comparison with pulmonary function tests and SPECT ventilation images. *Int J Radiat Oncol Biol Phys* 2014;90:414–422. [PubMed: 25104070]
10. Mathew L, Wheatley A, Castillo R, et al. Hyperpolarized He-3 magnetic resonance imaging: Comparison with four-dimensional x-ray computed tomography imaging in lung cancer. *Acad Radiol* 2012;19:1546–1553. [PubMed: 22999648]
11. Kipritidis J, Siva S, Hofman MS, et al. Validating and improving CT ventilation imaging by correlating with ventilation 4D-PET/CT using 68Ga-labeled nanoparticles. *Med Phys* 2014;41:011910. [PubMed: 24387518]
12. Brennan D, Schubert L, Diot Q, et al. Clinical validation of 4-dimensional computed tomography ventilation with pulmonary function test data. *Int J Radiat Oncol Biol Phys* 2015;92:423–429. [PubMed: 25817531]
13. Vinogradskiy Y, Castillo R, Castillo E, et al. Use of 4-dimensional computed tomography-based ventilation imaging to correlate lung dose and function with clinical outcomes. *Int J Radiat Oncol Biol Phys* 2013;86:366–371. [PubMed: 23474113]
14. Yaremko BP, Guerrero TM, Noyola-Martinez J, et al. Reduction of normal lung irradiation in locally advanced non-small-cell lung cancer patients, using ventilation images for functional avoidance. *Int J Radiat Oncol Biol Phys* 2007;68:562–571. [PubMed: 17398028]
15. Yamamoto T, Kabus S, von Berg J, et al. Impact of four-dimensional computed tomography pulmonary ventilation imaging-based functional avoidance for lung cancer radiotherapy. *Int J Radiat Oncol Biol Phys* 2011;79:279–288. [PubMed: 20646852]
16. Kimura T, Doi Y, Nakashima T, et al. Combined ventilation and perfusion imaging correlates with the dosimetric parameters of radiation pneumonitis in radiation therapy planning for lung cancer. *Int J Radiat Oncol Biol Phys* 2015;93:778–787. [PubMed: 26530746]

17. Yamamoto T, Kabus S, von Berg J, et al. Impact of four-dimensional CT-derived pulmonary ventilation images on radiotherapy treatment planning for lung cancer. *Int J Radiat Oncol Biol Phys* 2009;75:S443; S443.
18. Ireland RH, Tahir BA, Wild JM, et al. Functional image-guided radiotherapy planning for normal lung avoidance. *Clin Oncol (R Coll Radiol)* 2016;28:695–707. [PubMed: 27637724]
19. Marks LB, Sherouse GW, Munley MT, et al. Incorporation of functional status into dose-volume analysis. *Med Phys* 1999;26:196–199. [PubMed: 10076973]
20. Marks LB, Spencer DP, Bentel GC, et al. The utility of SPECT lung perfusion scans in minimizing and assessing the physiological consequences of thoracic irradiation. *Int J Radiat Oncol Biol Phys* 1993; 26:659–668. [PubMed: 8330998]
21. Siva S, Hardcastle N, Kron T, et al. Ventilation/perfusion positron emission tomography—based assessment of radiation injury to lung. *Int J Radiat Oncol Biol Phys* 2015;93:408–417. [PubMed: 26275510]
22. Ireland RH, Bragg CM, McJury M, et al. Feasibility of image registration and intensity-modulated radiotherapy planning with hyper-polarized helium-3 magnetic resonance imaging for non—small-cell lung cancer. *Int J Radiat Oncol Biol Phys* 2007;68:273–281. [PubMed: 17448880]
23. Faught AM, Miyasaka Y, Kadoya N, et al. Evaluating the toxicity reduction with CT-ventilation functional avoidance radiotherapy. *Int J Radiat Oncol Biol Phys* 2017;99:325–333. [PubMed: 28871982]
24. Lind PA, Marks LB, Hollis D, et al. Receiver operating characteristic curves to assess predictors of radiation-induced symptomatic lung injury. *Int J Radiat Oncol Biol Phys* 2002;54:340–347. [PubMed: 12243806]
25. Lan F, Jeudy J, Senan S, et al. Should regional ventilation function be considered during radiation treatment planning to prevent radiation-induced complications? *Med Phys* 2016;43:5072–5079. [PubMed: 27587037]
26. Yamamoto T, Kabus S, Bal M, et al. The first patient treatment of computed tomography ventilation functional image-guided radiotherapy for lung cancer. *Radiother Oncol* 2016;118:227–231. [PubMed: 26687903]
27. Marks LB, Bentzen SM, Deasy JO, et al. Radiation dose-volume effects in the lung. *Int J Radiat Oncol Biol Phys* 2010;76:S70–S76. [PubMed: 20171521]
28. Kadoya N, Cho SY, Kanai T, et al. Dosimetric impact of 4-dimensional computed tomography ventilation imaging-based functional treatment planning for stereotactic body radiation therapy with 3-dimensional conformal radiation therapy. *Pract Radiat Oncol* 2015;5:e505–e512. [PubMed: 25899221]
29. Vinogradskiy YY, Castillo R, Castillo E, et al. Use of weekly 4dct-based ventilation maps to quantify changes in lung function for patients undergoing radiation therapy. *Med Phys* 2012;39:289–298. [PubMed: 22225299]
30. Castillo E, Castillo R, White B, et al. Least median of squares filtering of locally optimal point matches for compressible flow image registration. *Phys Med Biol* 2012;57:4827–4843. [PubMed: 22797602]
31. Simon BA. Non-invasive imaging of regional lung function using x-ray computed tomography. *J Clin Monit Comput* 2000;16:433–442. [PubMed: 12580227]
32. Faught AM, Yamamoto T, Castillo R, et al. Evaluating which dose-function metrics are most critical for functional-guided radiotherapy with CT ventilation imaging. *Int J Radiat Oncol Biol Phys* 2017;99:202–209. [PubMed: 28816147]
33. Waxweiler T, Schubert L, Diot Q, et al. A complete 4dct-ventilation functional avoidance virtual trial: Developing strategies for prospective clinical trials. *J Appl Clin Med Phys* 2017;18:144–152.
34. Parker JA, Coleman RE, Grady E, et al. SNM practice guideline for lung scintigraphy 4.0. *J Nucl Med Technol* 2012;40:57–65. [PubMed: 22282651]
35. Siva S, Thomas R, Callahan J, et al. High-resolution pulmonary ventilation and perfusion PET/CT allows for functionally adapted intensity modulated radiotherapy in lung cancer. *Radiother Oncol* 2015;115:157–162. [PubMed: 25935743]

36. Huang T-C, Hsiao C-Y, Chien C-R, et al. IMRT treatment plans and functional planning with functional lung imaging from 4D-CT for thoracic cancer patients. *Radiat Oncol* 2013;8:3. [PubMed: 23281734]
37. Christian JA, Partridge M, Nioutsikou E, et al. The incorporation of spect functional lung imaging into inverse radiotherapy planning for non-small cell lung cancer. *Radiother Oncol* 2005;77:271–277. [PubMed: 16274762]
38. Munawar I, Yaremko BP, Craig J, et al. Intensity modulated radiotherapy of non-small-cell lung cancer incorporating SPECT ventilation imaging. *Med Phys* 2010;37:1863–1872. [PubMed: 20443508]
39. Simon R Optimal two-stage designs for phase II clinical trials. *Control Clin Trials* 1989;10:1–10. [PubMed: 2702835]
40. Sura S, Gupta V, Yorke E, et al. Intensity-modulated radiation therapy (IMRT) for inoperable non-small cell lung cancer: The Memorial Sloan-Kettering Cancer Center (MSKCC) experience. *Radiother Oncol* 2008;87:17–23. [PubMed: 18343515]
41. Liao Z, Mohan R, Xu T, et al. Comparing risk of radiation pneumonitis after intensity-modulated radiotherapy vs. proton therapy. *Int J Radiat Oncol Biol Phys* 2014;90:S42.
42. Briere TM, Krafft S, Liao Z, et al. Lung size and the risk of radiation pneumonitis. *Int J Radiat Oncol Biol Phys* 2016;94:377–384. [PubMed: 26675062]
43. Yom SS, Liao Z, Liu HH, et al. Initial evaluation of treatment-related pneumonitis in advanced-stage non—small-cell lung cancer patients treated with concurrent chemotherapy and intensity-modulated radiotherapy. *Int J Radiat Oncol Biol Phys* 2007;68:94–102. [PubMed: 17321067]
44. Bradley JD, Paulus R, Komaki R, et al. Standard-dose versus high-dose conformal radiotherapy with concurrent and consolidation carboplatin plus paclitaxel with or without cetuximab for patients with stage IIIa or IIIb non-small-cell lung cancer (RTOG 0617): A randomised, two-by-two factorial phase 3 study. *Lancet Oncol* 2015; 16:187–199. [PubMed: 25601342]
45. Chun SG, Hu C, Choy H, et al. Impact of intensity-modulated radiation therapy technique for locally advanced non—small-cell lung cancer: A secondary analysis of the NRG oncology RTOG 0617 randomized clinical trial. *J Clin Oncol* 2016;35:56–62. [PubMed: 28034064]
46. Faivre-Finn C, Snee M, Ashcroft L, et al. Concurrent once-daily versus twice-daily chemoradiotherapy in patients with limited-stage small-cell lung cancer (convert): An open-label, phase 3, randomised, superiority trial. *Lancet Oncol* 2017;18: 1116–1125. [PubMed: 28642008]
47. Komaki RU, Wei X, Allen PK, et al. Factors associated with severe pneumonitis for limited stage small cell lung cancer. *Int J Radiat Oncol Biol Phys* 2015;93:E436–E437.
48. St-Hilaire J, Lavoie C, Dagnault A, et al. Functional avoidance of lung in plan optimization with an aperture-based inverse planning system. *Radiother Oncol* 2011;100:390–395. [PubMed: 21963286]
49. Yamamoto T, Kabus S, Lorenz C, et al. 4D CT lung ventilation images are affected by the 4D CT sorting method. *Med Phys* 2013; 40:101907. [PubMed: 24089909]
50. Tucker SL, Liu HH, Liao ZX, et al. Analysis of radiation pneumonitis risk using a generalized Lyman model. *Int J Radiat Oncol Biol Phys* 2008;72:568–574. [PubMed: 18793959]
51. Yamamoto T, Kabus S, Klinder T, et al. Four-dimensional computed tomography pulmonary ventilation images vary with deformable image registration algorithms and metrics. *Med Phys* 2011;38:1348–1358. [PubMed: 21520845]
52. Du K, Reinhardt JM, Christensen GE, et al. Respiratory effort correction strategies to improve the reproducibility of lung expansion measurements. *Medical Phys* 2013;40:123504.
53. Kipritidis J, Cazoulat G, Tahir B, et al. The vampire challenge: Results of an international multi-institutional validation study to evaluate CT ventilation imaging algorithms: TH-EF-605–04. *Med Phys* 2017;44:3311.

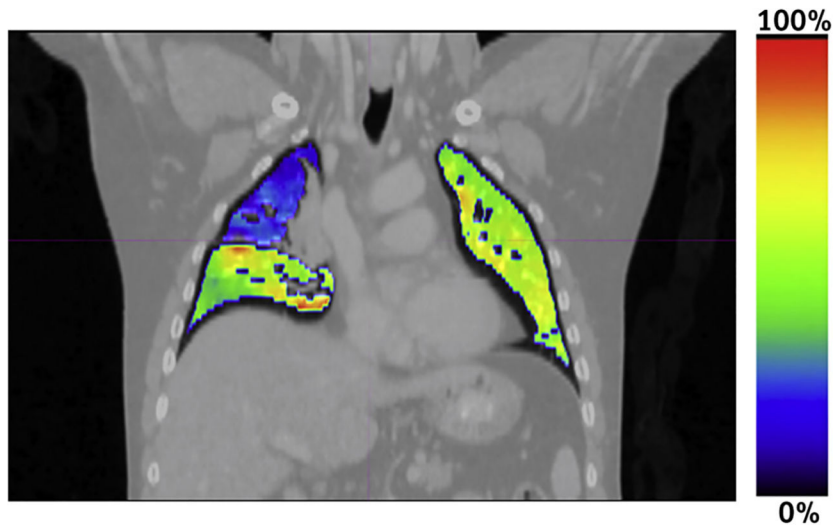


Fig. 1. An example of a 4-dimensional computed tomography—ventilation image overlaid with a standard computed tomography image. The color grading scale represents ventilation values calculated using Equation 1 that have been scaled to a percentage. The bright colors represent functional lung, and the blue and darker tones represent regions of ventilation defect. The presented patient has a ventilation defect in the right upper lobe.

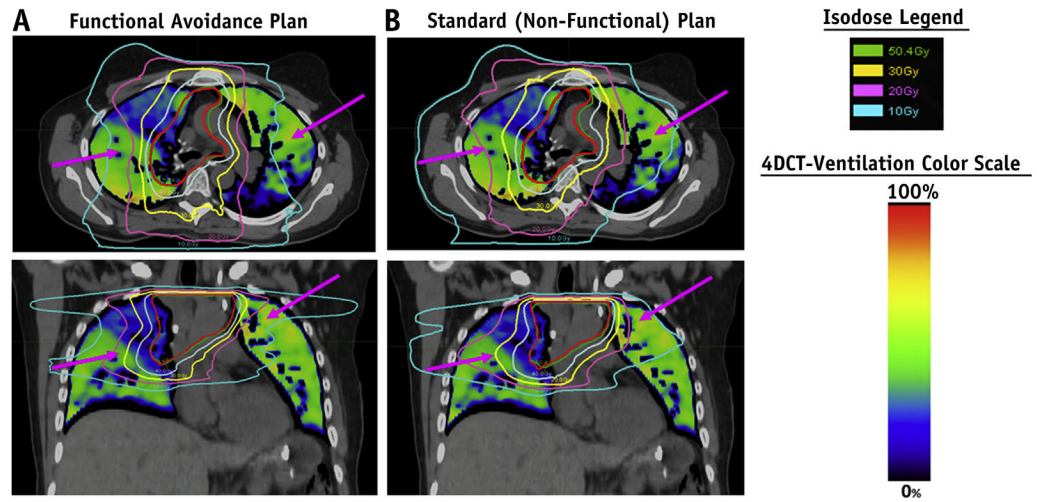


Fig. 2. An example case of a large difference in dose to functional lung (as measured by 4-dimensional computed tomography—ventilation) between the functional avoidance plan (A) and a nonfunctional plan (B). The computed tomography, 4-dimensional computed tomography—ventilation images, isodose lines, and planning target volume (shown in red) are presented for both plans. The arrows highlight the regions with the most prevalent functional lung sparing.

Author Manuscript

Author Manuscript

Author Manuscript

Author Manuscript

Table 1

Clinical parameters of study cohort

Parameter	n (%) or median (range)
Number of patients	17
Sex	
Female	13 (76)
Male	4 (24)
COPD	
Yes	6 (35)
No	11 (65)
Prior surgery	
Yes	5 (29)
No	12 (71)
Smoking status	
Nonsmokers	1 (6)
Current smokers	5 (29)
Former smokers	11 (65)
KPS index	90 (80–100)
Type of lung cancer	
NSCLC	12 (71)
SCLC	5 (29)
Stage	
IIA	2 (12)
IIB	0 (0)
IIIA	10 (59)
IIIB	4 (23)
IV	1 (6)

Abbreviations: COPD = chronic obstructive pulmonary disease; KPS = Karnofsky Performance Status; NSCLC = non-small cell lung cancer; SCLC = small cell lung cancer.

Table 2

Dosimetric results for the functional avoidance trial cohort

Parameter	Functional avoidance plan:	Nonfunctional plan:	<i>t</i> test
	Mean \pm SD	Mean \pm SD	<i>P</i> value
PTV coverage of Rx dose (%)	95.0 \pm 4.5	96.0 \pm 5.7	.04
PTV hotspot (%)	20.5 \pm 10.8	19.0 \pm 11.1	.06
Mean lung dose (Gy)	14.4 \pm 3.4	15.3 \pm 3.3	<.01
Lung V20 (%)	24.5 \pm 7.2	26.3 \pm 7.1	<.01
Maximum spinal cord dose (Gy)	34.9 \pm 7.9	33.6 \pm 8.2	.05
Mean esophagus dose (Gy)	23.2 \pm 8.1	23.9 \pm 7.6	.01
Mean heart dose (Gy)	11.2 \pm 8.3	11.1 \pm 8.0	.37
Functional avoidance structure			
Mean (Gy)	13.4 \pm 3.8	14.8 \pm 3.3	<.01
V5 (%)	67.3 \pm 17.4	71.0 \pm 14.6	<.01
V10 (%)	42.3 \pm 13.9	50.1 \pm 16.3	<.01
V20 (%)	21.6 \pm 9.5	24.8 \pm 9.4	<.01
V30 (%)	12.3 \pm 6.3	14.3 \pm 7.0	<.01

Abbreviations: PTV = planning target volume; Rx = prescription; SD = standard deviation; V5, V10, V20, or V30 = percentage of structure volume receiving 5-Gy, 10-Gy, 20-Gy, or 30-Gy doses, or higher doses.

Seventeen patients were included in the dosimetric analysis. Dosimetry for nonfunctional plans is shown for reference.

Table 3

Thoracic clinical toxicity adverse events for the interim analysis cohort (17 patients)

Adverse event	Grade 0 n (%)	Grade 1 n (%)	Grade 2 n (%)	Grade 3 n (%)
Pneumonitis	6 (35.3)	8 (47.1)	2 (11.8)	1 (5.9)
Esophagitis	1 (5.9)	8 (47.1)	6 (35.3)	2 (11.8)
Dyspnea	5 (29.4)	5 (29.4)	7 (41.2)	0 (0.0)
Cough	4 (23.5)	10 (58.8)	3 (17.6)	0 (0.0)
Fatigue	3 (17.6)	13 (76.5)	1 (5.9)	0 (0.0)

Number of patients and percentage is reported for each adverse event and toxicity grade.

Author Manuscript

Author Manuscript

Author Manuscript

Author Manuscript